Macrophage metalloproteinases degrade high-density-lipoprotein-associated apolipoprotein A-I at both the N- and C-termini

Ivano EBERINI*, Laura CALABRESI†, Robin WAIT‡, Gabriella TEDESCHI§, Angela PIRILLO*, Lina PUGLISI*, Cesare R. SIRTORI*† and Elisabetta GIANAZZA*[1]

*Dipartimento di Scienze Farmacologiche, Università degli Studi di Milano, via G. Balzaretti, 9, I-20133 Milano, Italy, †Centro E. Grossi Paoletti per lo Studio delle Dislipidemie, Dipartimento di Scienze Farmacologiche, Università degli Studi di Milano, via G. Balzaretti, 9, I-20133 Milano, Italy, ‡Kennedy Institute of Rheumatology Division, Faculty of Medicine, Imperial College of Science, Technology and Medicine, 1 Aspenlea Road, Hammersmith, London W6 8LH, U.K., and §Dipartimento di Patologia Animale, Igiene e Sanità Pubblica Veterinaria, Sezione di Biochimica, Università degli Studi di Milano, via G. Celoria, 12, I-20133 Milano, Italy

Atheromatous plaques contain various cell types, including macrophages, endothelial cells and smooth-muscle cells. To investigate the possible interactions between secreted matrix metalloproteinases and high-density lipoprotein (HDL) components, we tested the above cell types by culturing them for 24 h. HDL_3 (HDL subfractions with average sizes of between 8.44 nm for HDL_{3A} and 7.62 nm for HDL_{3C}) were then incubated in their cell-free conditioned media. Proteolytic degradation of apolipoprotein A-I was observed with macrophages, but not with endothelial-cell- or muscle-cell-conditioned supernatant. Absence of calcium or addition of EDTA to incubation media prevented all proteolytic processes. The identified apolipoprotein A-I fragments had sizes of 26, 22, 14 and 9 kDa. Two-dimensional electrophoresis and MS resolved the 26 and the 22 kDa components and identified peptides resulting from both N- and C-terminal cleavage of apolipoprotein A-I. The higher abundance of C- than N-terminally cleaved peptides agrees with data in the literature for a fully structured α-helix around Tyr^{18} compared with an unstructured region around Gly^{185} and Gly^{186}. The flexibility in the latter region of apolipoprotein A-I may explain its susceptibility to proteolysis. In our experimental set-up, HDL_{3C} was more extensively degraded than the other HDL_3 subclasses (HDL_{3A} and HDL_{3B}). Proteolytic fragments produced by metalloproteinase action were shown by gel filtration and electrophoresis to be neither associated with lipids nor self-associated.

Key words: atherosclerosis, mass spectrometry, matrix metalloproteinase, proteolysis, two-dimensional electrophoresis.

INTRODUCTION

Matrix metalloproteinases (MMPs), a family of calcium- and zinc-dependent endoproteinases with catalytic activity against extracellular matrix components [1], have been implicated in the progression of atherosclerotic plaques. In their active form they may contribute to vascular remodelling [migration and proliferation of smooth-muscle cells (SMCs) with neointima formation] and plaque disruption [2–5]. *Ex-vivo*, MMP-2 can be detected histochemically in normal human arteries together with its inhibitors, tissue inhibitor of metalloproteinases (TIMP)-1 and TIMP-2. In atheromas, on the contrary, MMP-9 and MMP-3 are associated mainly with SMCs, MMP-1 with endothelial cells, and all of the above with foam cells [6]. SMCs can also produce three membrane MMPs (MT1-MMP, MT2-MMP and MT3-MMP) [7]; MT1 is believed to be the physiological activator of MMP-2 [8]. Several factors and mediators associated with the atherosclerotic plaque influence MMP levels.

All cell types involved in atherosclerotic plaque formation have been reported to release MMPs. Cultured SMCs constitutively produce MMP-2 and TIMP. After interleukin 1 or tumour necrosis factor α (TNF-α), MMP-9, MMP-3 and MMP-1 are also expressed, whereas the level of TIMPs is unaffected [6]. Human macrophages produce MMP-1, MMP-3 [9], MMP-9 [10] and MMP-12 [11], and fibroblasts produce MMP-2 [12]. After stimulation with lipopolysaccharide (LPS), mouse macrophages express TNF-α and MMPs 2 and 9 [13].

One investigation focused on a possible role for MMPs in atherogenesis, when cholesterol accumulates in the cells of arterial intima [14]. After incubation with MMPs 3, 7 or 12, the ability of high-density lipoprotein $(HDL)_3$ (HDL subfractions with average sizes of between 8.44 nm for HDL_{3A} and 7.62 nm for HDL_{3C}) to induce the high-affinity component of cholesterol efflux from macrophage foam cells is markedly decreased, whereas preincubation with MMP-1 reduces cholesterol efflux only slightly and MMP-9 is ineffective [14]. The effects of the various MMPs appear to be reflected in their differential abilities to degrade small preβ-migrating particles present in the HDL_3 fraction: MMPs that strongly reduce cholesterol efflux cleave the C-terminal region of apolipoprotein A-I (apoA-I) and produce a major fragment of about 22 kDa [14].

The above results were obtained in an *in vitro* system, with the use of recombinant MMPs, often after short incubation times and in the presence of high protease-to-substrate ratios [14]. The present investigation had, therefore, the following aims: (i) to test the ability of MMPs, produced by different cell lines, to

Abbreviations used: apoA-I, apolipoprotein A-I; GGE, gradient gel electrophoresis; HDL, high-density lipoprotein; HUVEC, human umbilical vein endothelial cell; IPG, immobilized pH gradient; MMP, matrix metalloproteinase; 2-DE, two-dimensional electrophoresis; LPS, lipopolysaccharide; PAA, polyacrylamide; RPM, rat peritoneal macrophage; SMC, smooth-muscle cell; TIMP, tissue inhibitor of metalloproteinases; TNF-α, tumour necrosis factor α.

[1] To whom correspondence should be addressed (e-mail Elisabetta.Gianazza@unimi.it).

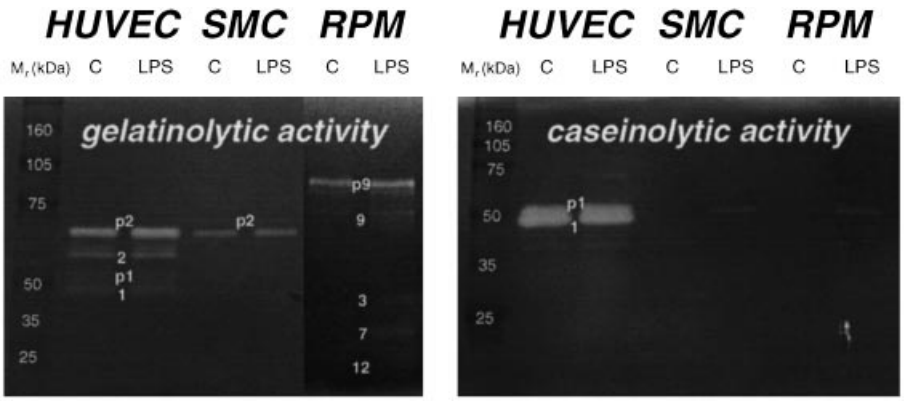

Figure 1 Gelatinolytic and caseinolytic activities in cell-culture supernatants

Media conditioned for 24 h from HUVECs, SMCs and RPMs in culture with (LPS) or without (C) LPS stimulation. Aliquots of 40 μl from each supernatant were resolved by SDS/PAGE on 7.5%T PAA in Tris/HCl//Tris/glycine buffer in the presence of 1 mg/ml gelatin or on commercial 10%T PAA gels containing casein. After washing with 2.5% Triton X-100 in saline, the gel slabs were incubated for 24 h at 37 °C in Tris/HCl, pH 7.5, containing 10 mM $CaCl_2$ and 3 μM $ZnCl_2$, and stained with Coomassie Brilliant Blue. Numbers on the gels refer to MMP classification (e.g. 1 = MMP-1); p means proenzymic form (e.g. p1 = proMMP-1).

degrade HDL_3 under approximately physiological conditions; (ii) to detect and characterize all digestion fragments by a variety of analytical techniques and (iii) to verify the consistency between our findings and published structural data and models.

In our experiments, HDL_3 was incubated for up to 72 h in supernatants from the cultures of the three cell types most common in vascular walls and atherosclerotic plaques, namely endothelial cells, SMCs and macrophages. Lipoproteins, apolipoproteins and their fragments were then fractionated by electrophoretic methods and characterized by biochemical, immunological and MS techniques.

EXPERIMENTAL

Lipoproteins

The HDL_3 subfraction was separated from plasma of healthy donors by sequential flotation on KBr [15] and dialysed against PBS containing 0.01 % (w/v) sodium EDTA.

Cell culture and MMP activity testing

Rat peritoneal macrophages (RPMs) were collected from control Sprague–Dawley rats by lavage with cold PBS and plated at a density of 1×10^6 cells/ml, or in one case 2×10^6 cells/ml. Human umbilical vein endothelial cells (HUVECs) and SMCs from rat aorta were grown until subconfluence. Medium 199 with or without 10 μg/ml LPS or, in some cases, 40–500 units/ml TNF-α, was conditioned for 24 h with each cell line. In order to avoid interference from serum proteases and protease inhibitors, the medium did not contain fetal calf serum, except for HUVEC cultures, which contained residues of fetal calf serum from previous culture steps that were not rinsed away. The culture supernatants collected after centrifugation at 4 °C for 20 min at 1500 ***g*** were tested for gelatinolytic and caseinolytic activities.

Lipoprotein treatment

The culture supernatants were made to 10 mM $CaCl_2$, then 400 μg/ml HDL_3 was added and incubation was allowed to proceed for up to 72 h at 37 °C. Residual HDL_3 was characterized using a combination of electrophoretic techniques.

Electrophoresis

All experiments were performed under non-reducing conditions. Lipoprotein size was assessed by migration on 4–30 %T (where %T is the total monomer concentration in g/100 ml) polyacrylamide (PAA) gradients in Tris/borate/EDTA [16]. The pI values of apolipoproteins were evaluated by focusing on a non-linear 4–10 immobilized pH gradient (IPG) [17] in the presence of 8 M urea, and their M_r values estimated by SDS/PAGE on 10–22 %T PAA in Tris/HCl//Tris/tricine buffer [18]. Two-dimensional electrophoresis (2-DE) was performed through a sequence of the above steps [19]. For qualitative evaluation and MS analysis the protein patterns were stained with either Coomassie Brilliant Blue or silver nitrate [20]; for immunological detection and N-terminal sequencing the proteins were electroblotted to either nitrocellulose in Tris/glycine buffer or to PVDF in 3-(cyclohexylamino)propanesulphonic acid (Caps)/NaOH. Spot volumes in 2-DE patterns were quantified using PDQUEST (Bio-Rad, Hercules, CA, U.S.A.). Immunological detection was with a polyclonal anti-apoA-I antiserum followed by horseradish peroxidase-conjugated anti-rabbit IgG and ECL zymography. The assortment of apolipoproteins and their fragments in the various HDL_3 subclasses was investigated by a non-conventional two-dimensional electrophoretic technique, including migration on a 4–25 %T PAA gradient in Tris/borate/EDTA, for either 75 min or 24 h, and SDS/PAGE on 10–22 %T PAA as above.

Matrix-assisted laser-desorption ionization MS

In-gel digestion with trypsin was performed according to published methods [21–23]. Matrix-assisted laser-desorption ionization mass spectra were recorded with a TofSpec 2E spectrometer (Micromass, Manchester, U.K.) equipped with a 337 nm nitrogen laser. The instrument was operated in the positive-ion reflectron mode at 20 kV accelerating voltage with time-lag focusing enabled. The matrix was a mixture of α-cyano-4-hydroxy-cinnamic acid and nitrocellulose [24]. For electrospray ionization experiments, desalted samples were loaded into palladium-coated borosilicate nanoelectrospray needles (Protana, Odense, Denmark) and mounted in the source of a

Q-Tof hybrid quadrupole/orthogonal acceleration time-of-flight spectrometer (Micromass).

N-terminal sequencing

Automated sequence analysis was performed on a pulsed-liquid sequencer (model 477; Applied Biosystems, Foster City, CA, U.S.A.) equipped with a 120A Applied Biosystems PTH analyser.

Gel filtration

A 4 ml sample of HDL_3, after a 3 day incubation in RPM supernatant, was fractionated by size on three serial Superose 6B columns (1.6 cm × 100 cm; Amersham Bioscience, Uppsala, Sweden), equilibrated in 10 mM Tris/HCl, pH 7.4, with 150 mM NaCl and 0.01 % EDTA. The flow rate was 0.18 ml/min; the first 150 ml was discarded and fractions of 2 ml were collected. Aliquots of the eluate were analysed by SDS/PAGE, as above.

Phospholipid quantification

Phospholipid levels were determined by the enzymic method [25].

RESULTS

Figure 1 shows the zymograms for proteolytic activity (gelatinolytic, left-hand panel; caseinolytic, right-hand panel) on the supernatants after 24 h culture of HUVECs, SMCs and RPMs, without stimulation and after treatment with 10 μg/ml LPS. In all cases the amounts of secreted proteases and the ratios between proforms and mature forms were affected only to a minimal extent by LPS treatment; the same lack of effect on the above parameters was also observed with TNF-α treatment (50–400 units/ml [26]; results not shown).

Most proteases expressed by the three cell types have gelatin as their preferential substrate. SMCs and HUVECs both release MMP-2, while the latter cell line is the main producer of a caseinolytic enzyme identified as MMP-1. The major proteolytic enzymes secreted by RPMs are MMP-9 and MMP-12, with some MMP-3 and MMP-7 also being expressed.

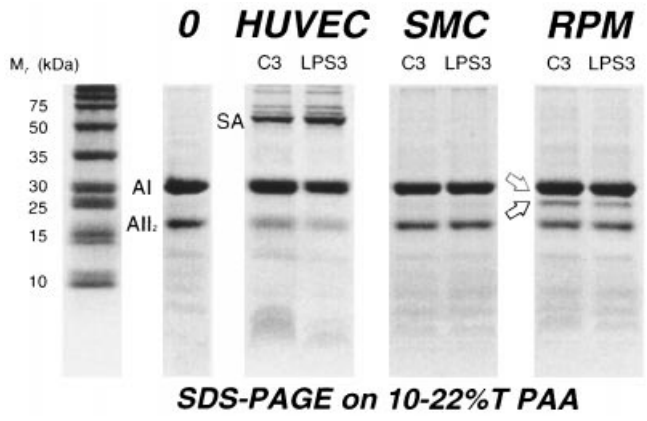

Figure 2 ApoA-I proteolysis after a 3 day incubation of HDL_3 in cell-culture supernatants

From left to right: molecular-mass markers, control HDL_3 (0) and HDL_3 incubated in HUVEC-, SMC- and RPM-conditioned media. The latter three were with (LPS) or without (C) LPS stimulation. SDS/PAGE on 10–22%T PAA gradient in Tris/HCl//Tris/tricine buffer (10 μg of protein/lane). The black and grey arrows point, respectively, to a resolved peptide and to the position of further unresolved proteolytic fragments. AI, apoA-I; AII_2, dimeric apoA-II; SA, contaminating albumin.

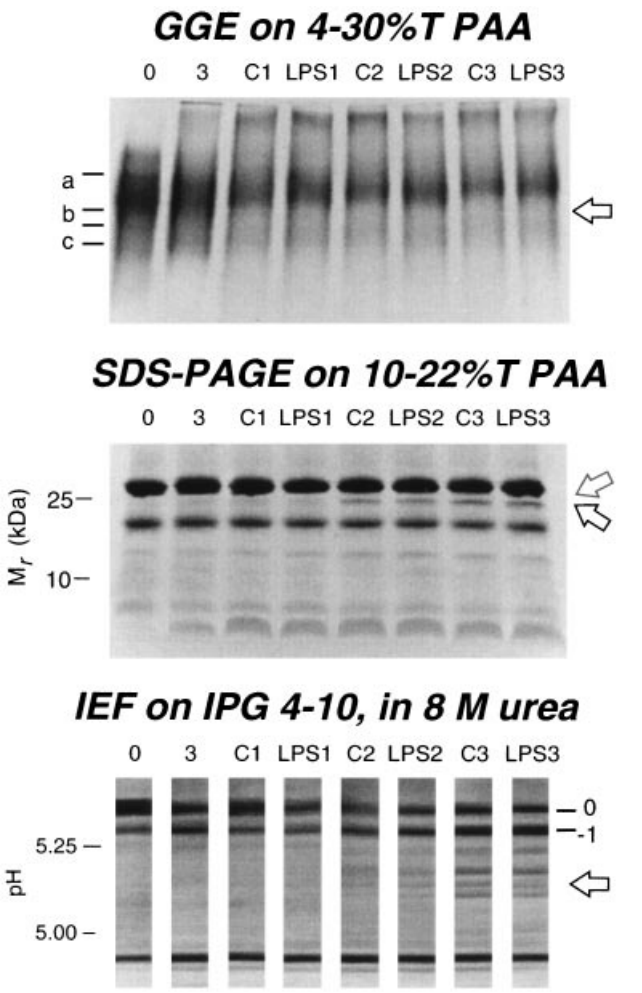

Figure 3 Time course of HDL_3 and apoA-I modifications upon incubation in RPM-conditioned medium

Top panel: GGE on 4–30%T PAA in Tris/borate/EDTA. a, b and c refer to HDL_{3A-3C}. Middle panel: SDS/PAGE on 10–22%T PAA gradient in Tris/HCl//Tris/tricine buffer under non-reducing conditions. Bottom panel: isoelectric focusing (IEF) on a 4–10 IPG in the presence of 8 M urea, under non-reducing conditions. From left to right: lipoproteins in non-conditioned medium, before (0) or after (3) incubation 3 days at 37 °C; lipopoproteins incubated for an increasing length of time (1–3 days) at 37 °C in RPM-conditioned medium with (LPS) or without (C) 10 μg/ml LPS stimulation. The three panels are cropped from larger images. Black and grey arrows are as in Figure 2.

Figure 2 compares the SDS/PAGE patterns of HDL_3 after a 3 day incubation in medium conditioned for 24 h by HUVECs, SMCs or RPMs, with and without the addition of 10 μg/ml LPS, with that of normal HDL_3. The major lipoprotein components (apoA-I and dimeric apoA-II) are marked, together with contaminating albumin in HUVEC supernatants. No change in apoA-II concentration was detected in any sample. The black arrow points to a proteolytic fragment with a mass of approx. 22 kDa, most probably derived from apoA-I and found in RPM samples. Figure 4 (see below) demonstrates in RPM-conditioned medium the presence of further proteolytic fragments, about 26 kDa in size, which failed to be resolved by one-dimensional electrophoresis at high sample loads (Figure 2, grey arrow). HDL_3 incubation in RPM-conditioned media without $CaCl_2$ or with $CaCl_2$ and EDTA failed to produce any protein digestion (results not shown). The MMPs that were newly secreted by

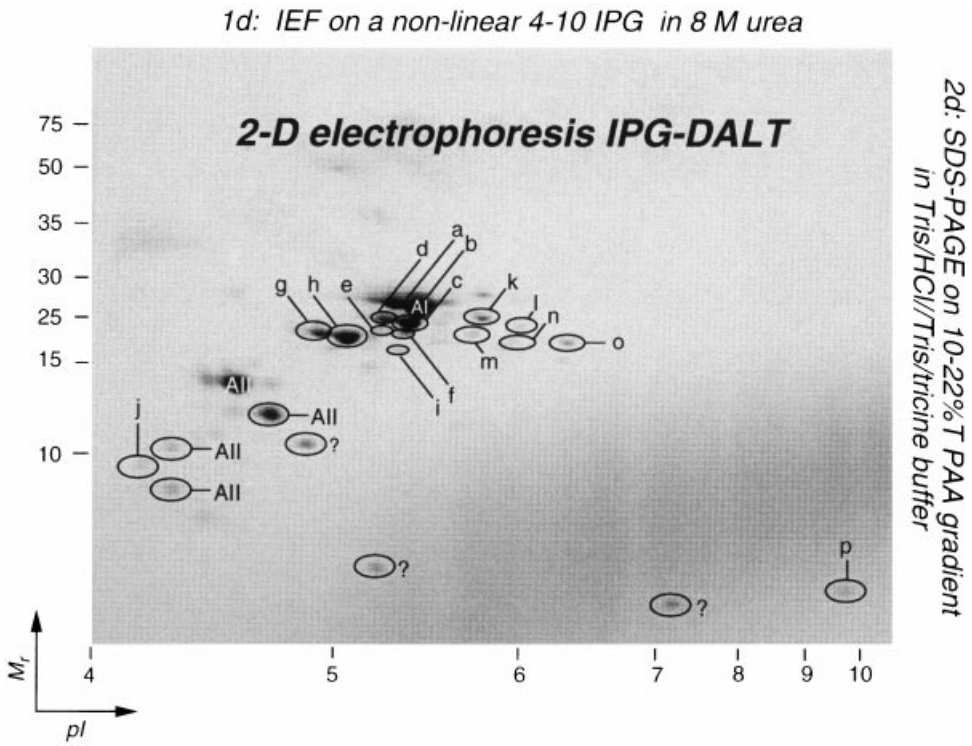

Figure 4 Structural characterization of proteolytic fragments after HDL_3 incubation in RPM-conditioned medium

After 3 days at 37 °C in medium 199 conditioned for 24 h with 2×10^6 cells/ml, lipoproteins were desalted and concentrated by trichloroacetic acid/acetone precipitation and subjected to 2-DE: isoelectric focusing (IEF) on a 4–10 IPG in the presence of 8 M urea followed by SDS/PAGE on a 10–22%T PAA gradient in Tris/HCl//Tris/tricine buffer. Proteins were then stained directly for spot excision and MS processing, or electroblotted on to PVDF for N-terminal sequencing.

RPMs after LPS treatment (Figure 1) did not modify the pattern of HDL digestion. The interpretation was that these MMPs were expressed minimally and were inactive on this specific substrate.

Figure 3 shows the changes in the electrophoretic pattern for HDL_3 and constituent apolipoproteins as a function of time of incubation in RPM-conditioned medium. Figure 3 (top panel) shows the results of a gradient gel electrophoresis (GGE) which allows the size of the lipoproteins to be evaluated. The smallest particles (HDL_{3c}, arrow) appeared to be selectively degraded with time. The small decrease in overall concentration between the 0 and 3 treatments is due to non-specific protein adsorption to a salt precipitate that forms upon addition of calcium to the cell-culture supernatant. The middle panel of Figure 3 shows an SDS/PAGE for assessing apolipoprotein size. The 22 kDa fragment (Figure 3, middle panel, black arrow) is the only resolved newly formed peptide, which accumulated with time. Figure 3 (bottom panel) shows isoelectric focusing of apolipoproteins, dissociated and denatured by the presence of 8 M urea. Incubation for 3 days in non-conditioned medium brought about a shift in the balance (Figure 3, bottom panel, lane 3 compared with lane 0) between the 0 and -1 isoforms of apoA-I, which differ by an Asn → Asp deamidation event [27]. Incubation in conditioned medium results in the appearance (Figure 3, bottom panel, lanes C3 and LPS3 compared with lane 0) of bands at a pI of approx. 5.15 (arrow).

Figure 4 shows the 2-DE map of a HDL_3 sample incubated for 3 days in medium 199 conditioned for 24 h with 2×10^6 RPMs/ml. The harsher digestion conditions, the higher protein load and the greater resolution of the analytical procedure allow for the identification of a large number of peptides. Some have a molecular mass of 26 kDa, which could not be resolved from the major apoA-I band in one-dimensional runs (see above). The peptides with mass values of approx. 22 kDa appear to be very heterogeneous in charge, whereas the densest spots are resolved at $pI < 5.25$, several minor components migrate at $pI > 5.25$. By densitometric evaluation of the 2-DE pattern (Table 1), the volume of apoA-I-derived peptides equals that of the intact parent protein, i.e. under these incubation conditions apoA-I has been degraded proteolytically by about 50%. A parallel analysis of an HDL_3 sample incubated for 3 days in medium 199 conditioned for 24 h by 1×10^6 RPMs/ml demonstrates a 20% proteolytic degradation of apoA-I (results not shown).

All resolved spots were processed using MS fingerprinting to assess their derivation from either apoA-I or apoA-II. For the most abundant components, N-terminal sequencing was also performed after blotting on to a PVDF membrane. The results of such analytical procedures are summarized in Table 1. Peptides cleaved at both the N- and C-termini were detected; the former with a higher pI, the latter with a lower pI than apoA-I. The identification of peptides with masses of approx. 14 and 6 kDa (by SDS/PAGE) as well as bands with pI values both lower and higher than the reference apoA-I (in isoelectric focusing) as apoA-I fragments was assessed further by immunoblotting procedures (results not shown).

The question of how cleaved apoA-I associates with lipoproteins was addressed in two ways; a specifically designed 2-DE set-up, with GGE followed by SDS/PAGE (Figure 5), and gel filtration followed by analytical SDS/PAGE (Figure 6).

A control sample and an HDL_3 sample incubated for 3 days in medium 199 conditioned for 24 h by 1×10^6 RPMs/ml were

Table 1 Relative abundance and peptide MS coverage of apoA-I proteolytic fragments as resolved by 2-DE

Spots refer to those shown in Figure 4. Under N-terminus (sequencing), the numbers indicate the first amino acid at the N-terminus of each fragment according to the sequence of intact apoA-I; this was amino acid no. 1 for two fragments (that are confirmed as only C-terminally cleaved) and amino acid no. 19 for another fragment (confirmed as N-terminally cleaved). Total spot volume (%) refers to the percentage abundance of individual fragments with respect to total apoA-I (intact + fragments) loaded in the gel.

Spot	N-terminus (sequencing)	Peptide coverage (MS)	Total spot volume (%)
Intact apoA-I			
a			18.4
b			30.1
			Total 48.5
pI < 5.27			
c	1	11–215	13.5
d		11–215	6.1
e		11–188	1.4
f		11–188	0.6
g		11–173	6.6
h	1	11–188	15.9
i		119–188	0.6
j		11–97	0.6
			Total 45.3
pI > 5.27			
k	19	24–226	2.7
l			0.4
m		24–215	0.8
n		97–206	0.5
o		97–226	1.3
p		196–239	0.4
			Total 6.2

compared by electrophoresis. Non-equilibrium GGE (75 min run, corresponding to the time required for the tracking dye to migrate the entire length of the gel) resolved two components in the RPM-conditioned sample whose sizes were estimated at 26 and 22 kDa (Figure 5, left-hand panel, arrows). On the contrary, when GGE was run under equilibrium conditions, i.e. for 24 h, the SDS/PAGE step failed to detect in the RPM-conditioned sample any of the apoA-I fragments (Figure 5, right-hand panel): the fast-migrating components could not be retained by the PAA meshwork (as for all proteins < 70 kDa in size) and were eluted with time to the anodic compartment.

This finding could be interpreted either as the 'pulling' of apoA-I fragments by the applied electric field out of the HDL particles or as their release in the incubation medium upon proteolysis. Size fractionation of the sample was repeated by gel filtration (Figure 6). Two protein-containing peaks were resolved, the major one (peak A) with the same elution volume as reference HDL_3 (Figure 6, top panels). Quantification of the collected fractions demonstrated that, contrary to peak A, protein in peak B is not associated with phospholipids (Figure 6, middle panel). SDS/PAGE showed peak A to contain mainly intact apoA-I and apoA-II, whereas in peak B both the approx. 26 and approx. 22 kDa protein fragments were found, at elution volumes of 188 and 192 ml respectively.

DISCUSSION

Limited proteolysis has been applied to the study of apoA-I in different types of HDL and reconstituted lipoprotein, for structural, topological and functional purposes. Maximal suscep-

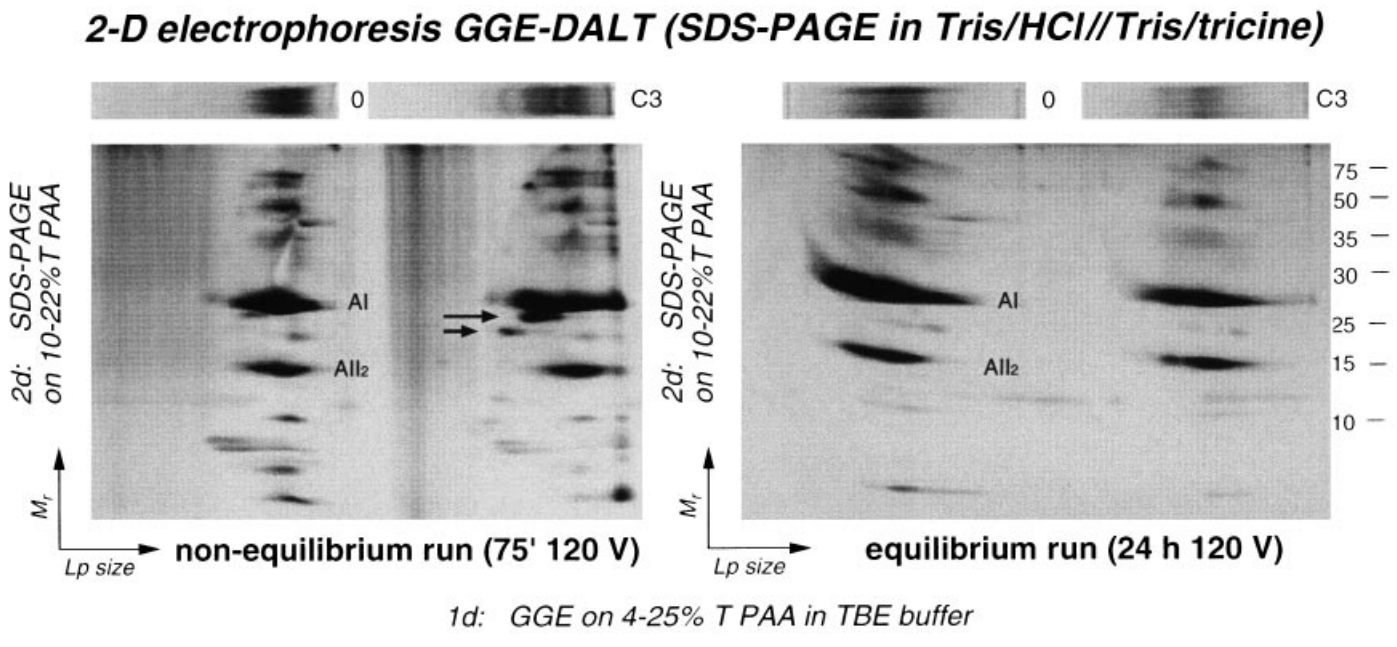

Figure 5 Assessment of the distribution of apoA-I, apoA-II and of their proteolytic fragments among the various HDL_3 subclasses

Control (0) and RPM-digested HDL_3 (C3) were separated by 4–25%T GGE either until the tracking dye migrated the entire length of the gel (75 min at 120 V in a 6 cm slab; left-hand panel) or until proteins reached their pore limit PAA concentration (24 h; right-hand panel); the Coomassie Brilliant Blue-stained patterns after this step are shown at the top. Gel strips from the GGE run (1 mm thick, cast on GelBond foil) were equilibrated in Tris/tricine/SDS buffer and embedded at right angles on 10–22%T PAA slabs for SDS/PAGE. The 2-DE protein pattern was stained with silver nitrate. Arrows point to approx. 26 and 22 kDa components, detectable in C3 compared with 0 after 75 min but lost in the anodic compartment after 24 h.

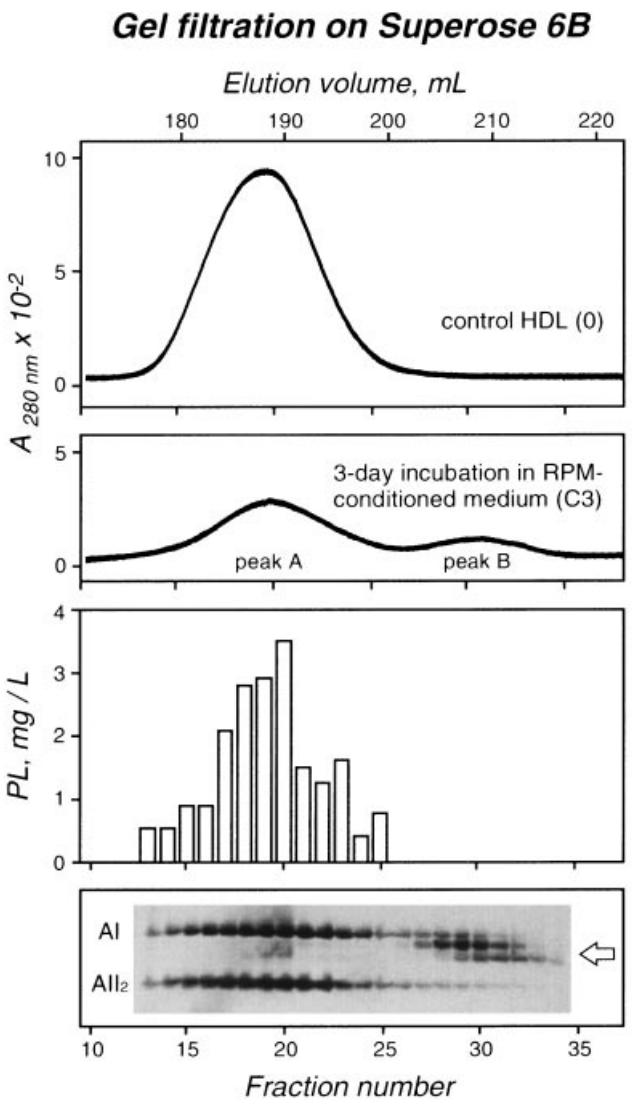

Figure 6 Discrimination between HDL_3-associated and free apolipoproteins/apolipoprotein fragments

Control (0) and RPM-digested HDL_3 (C3), approx. 1.5 mg/each, were eluted through a Superose B6 column. The two top panels show the A_{280} traces; the middle panel corresponds to the phospholipid (PL) content and the bottom panel to the SDS/PAGE pattern of the C3 fractions. Calibration is given in terms of both elution volume (top) and collected fractions (bottom).

tibility of lipid-bound apoA-I to proteolytic attack has been mapped in various experimental set-ups to the N-terminus [28,29], to the middle part [30–32] or to the C-terminus of the molecule [31–33]. This variability hints at major plasticity of apoA-I, whose conformation appears to depend on the size of the carrier particle, mode of reconstituted HDL preparation, type of added lipid and oxidation state of methionine residues.

The proteases used in the above tests, trypsin, chymotrypsin, V8 protease, elastase and chymase, were selected on the basis of their target site specificity, and have neither physiological nor pathological roles *in vivo* in (apo)lipoprotein processing and catabolism.

The report by Lindstedt et al. [14] dealing with the proteolytic activity of MMPs on apoA-I was the first investigation in which test proteases had an *in vivo* relevance, especially in relation to the onset and progression of atherosclerosis. Contrary to the situation in healthy arterial walls, in which the constitutive expression of MMP-2 is balanced by the presence of TIMPs, atheromas contain a variety of MMPs in their active form (MMPs 1, 2, 3, 9 and 11). Since lipoproteins and other serum components do enter the atheromatous lesion there is scope for enzyme–substrate interaction.

In the paper of Lindstedt et al. [14] recombinant MMPs were at high concentrations. In the present investigation, we tried to reproduce the assortment and relative concentration of MMPs in an 'atheromatous' environment, in the presence of MMP levels typical of cell-culture supernatants (around 1 μg/ml [34]).

Atheroma cells have morphological and functional properties different from their resting counterparts: SMCs display a secretory phenotype, epithelial cells a prothrombotic phenotype, whereas macrophages may turn into lipid-laden foam cells [35]. Different stimuli (TNF-α and LPS, in increasing concentrations) were applied to the cells in culture during the 24 h conditioning period. These treatments had only minimal effects on MMP production by the cell lines. This unresponsiveness is most likely linked to cell-culture conditions: RPMs as recruited in the peritoneal cavity were in an activated state, and unlike their behaviour in healthy vessels, SMCs and HUVECs were assayed when in a proliferating state.

It is remarkable that the MMPs with the greatest effect on apoA-I were secreted by macrophages, which are not typical components of the arterial wall but abundant in atheromatous lesions [35]. In contrast, neither smooth muscle nor endothelial cells released proteolytic enzymes able to interact with HDL_3. *In vivo*, apoA-I proteolysis by MMPs can thus be associated with atherosclerotic plaques from their onset onwards. After entering atheromatous lesions, apoA-I may compete with matrix components as a substrate for MMPs, and reduce the ability of arterial wall enzymes to effect remodelling and eventual plaque rupture. This could be part of the mechanism by which HDLs act as anti-atherogenic factors. However, MMP proteolytic action eventually inactivates HDL, particularly HDL_{3C}, the most efficient particles in removing cellular cholesterol [36]. Several authors (e.g. [14,37,38]) have already reported that proteolytic removal or mutation of the C-terminal region of apoA-I (amino acids 222–243) can reduce intracellular cholesterol efflux. Therefore lipid deposition in the early lesions cannot be limited further by this physiological protection mechanism.

Our data show clearly that, among HDL_3 subclasses, HDL_{3C} is degraded preferentially while, among HDL_3 components, apoA-I is a much more susceptible substrate than apoA-II. The reason for HDL_{3C} selective disruption could be ascribed to the relatively low lipid content in comparison with other HDL_3 subclasses (HDL_{3A} and HDL_{3B}). Indeed lipid-free apoA-I is degraded easily by proteolytic enzymes, with minimal selectivity in sequence targeting [33]. The extensive degradation of HDL_{3C} corresponds to the accumulation of massive amounts of proteolytic fragments: as resolved by 2-DE after 3 days of incubation, these amount to 20 % of total apoA-I-related material with samples from 1×10^6 RPMs/ml, and to 50 % with 2×10^6 RPMs/ml (Figure 4).

Two alternative theoretical models, based on amphipathic α-helices, have been proposed for the tertiary structure of lipid-bound apoA-I (residues 44–243). In the first, the picket-fence model of Phillips et al. [39], the helices run anti-parallel to one another (intramolecular protein–protein interactions) and parallel to the lipid acyl chains. In the second, the belt model of Segrest et al. [40], the helices run perpendicularly to phospholipids (intermolecular protein–protein interactions). A novel hairpin folding of each apoA-I monomer has been proposed, with

most helices perpendicular to the phospholipid acyl chains and a random head-to-tail and head-to-head arrangement of the two apoA-I molecules [41].

By scanning the primary sequence of apoA-I for the known target sites of MMPs and by computing the physico-chemical parameters of the resulting peptides with a module running on the ExPASy server (http://www.expasy.org/tools/pi_tool.html), we evaluated the pI for all fragments containing an intact N-terminus to be lower than 5.27, and for all fragments containing an intact C-terminus to be higher than 5.27, the pI of native apoA-I. Cuts near the N-terminus of the apoA-I molecule, despite being reported as occurring with other proteases [28,29], had not been described previously with MMPs [14]. The relative abundance of acidic compared with alkaline peptides, as listed in Table 1, demonstrates that, in a test medium closely resembling the situation *in vivo*, the C-terminal region of apoA-I is most susceptible to MMP digestion. Actually, alkaline peptides are found in appreciable amounts only under harsher experimental conditions, such as incubation in culture media conditioned with 2×10^6 RPMs/ml (comparison with incubation in different culture media not shown).

Reasons for greater susceptibility to proteolysis of the specified amino acid targets are probably related to topology. NMR data [42] on apoA-I(142–187), a peptide with a sequence identical to residues 142–187 of apoA-I, in either dodecylphosphocholine or SDS micelles, show the C-terminal region as unstructured due to the presence of Gly^{185} and Gly^{186}. On the contrary, diffraction data on Δ(1–43), a mutant lacking the indicated residues, crystallized in lipid-free form under high-salt conditions assigned the same region to an α-helix [43]. More recently the same authors reported a different crystallization protocol for Δ(1–43), including detergents in a low-ionic-strength solution, which resulted in a different structure [44] that is not yet resolved completely [45]. The accessibility to proteinases of susceptible bonds in the apoA-I C-terminal region, shown by our experiments, strengthens the hypothesis that amino acids around Tyr^{192} are not in a structured conformation.

In a recent NMR investigation, the structure of a C-terminally truncated form, Δ(187–243), assigned Tyr^{18} to an α-helix [46]; in agreement with the above discussion, this provides a hypothetical basis for the higher resistance to proteolysis of the N- versus the C-terminus in apoA-I under our experimental conditions.

Our data demonstrate that proteolytic fragments of apoA-I produced under the specified experimental conditions dissociate from lipids upon cleavage. These findings were unexpected in view of the current models of HDL structure (picket-fence [39] and belt [40]; see above), which assume the amphipatic α-helix to be the main motif in the secondary structure of this apolipoprotein. The driving force in determining HDL structure should then be the interaction between the phospholipid acyl chains and the amphipathic α-helices, spanning most of the protein sequence [47]. Assuming that a single cut in apoA-I would not cause very extensive α-helix unfolding, these data are difficult to account for, unless very strong co-operative binding is assumed. Our observations suggest a much higher affinity for lipids in the C-terminus: a cut in this region results in prompt dissociation of the 26 and 22 kDa fragments from HDL. Mutation of specific C-terminal hydrophobic residues have been reported to diminish the ability of apoA-I to bind to HDL [48].

The released fragments appear not to aggregate: in a gel chromatography set-up, the approx. 26 kDa component elutes before the approx. 22 kDa component (Figure 6), and their migration rate in a time course of non-equilibrium GGE versus dimeric apoA-I_{Milano} is suggestive of their being in monomeric form (results not shown). Indeed the C-terminal domain of apoA-I seems to be involved in the self-association of the protein [48].

We thank Dr F. Nardi for providing SMCs, Dr M. Camera and Ms F. Meloni for supplying HUVECs and Dr G. Chiesa, Dr E. Vegeto, Dr A. Cignarella (all from Dipartimento di Scienze Farmacologiche, Milan, Italy), Professor D. Spady (Southwestern Medical Center, University of Dallas, Dallas, TX, U.S.A.) and Professor I. J. Goldberg (Department of Medicine, Columbia University College of Physicians and Surgeons, New York, NY, U.S.A.) for stimulating discussion. This work was supported in part by grants from Università degli Studi di Milano (FIRST) and MURST (COFIN 2000–2001: Structural studies on hydrophobic molecule-binding proteins) to E.G., and a grant in aid by Esperion Therapeutics, Ann Arbor, MI, U.S.A.

REFERENCES

1 Woesser, J. F. and Nagase, H. (2000) Matrix Metalloproteinases and TIMPs, Oxford University Press, Oxford
2 Dollery, C. M., McEwan, J. R. and Henney, A. M. (1995) Matrix metalloproteinases and cardiovascular disease. Circ. Res. **77**, 863–868
3 Celentano, D. C. and Frishman, W. H. (1997) Matrix metalloproteinases and coronary artery disease: a novel therapeutic target. J. Clin. Pharmacol. **37**, 991–1000
4 Libby, P., Schoenbeck, U., Mach, F., Selwyn, A. P. and Ganz, P. (1998) Current concepts in cardiovascualr pathology: the role of LDL cholesterol in plaque rupture and stabilisation. Am. J. Med. **104**, 14S–18S
5 Pasterkamp, G., Schoneveld, A. H., Hijnen, D. J., de Klein, D. P. V., Teepen, H., van der Wal, A. C. and Borst, C. (2000) Atherosclerotic arterial remodeling and the localization of macrophages and matrix metalloproteases 1, 2 and 9 in the human coronary artery. Atherosclerosis **150**, 245–253
6 Galis, Z. S., Muszynski, M., Sukhova, G. K., Simon-Morrissey, E. and Libby, P. (1995) Enhanced expression of vascular matrix metalloproteinases induced *in vitro* by cytokines and in regions of human atherosclerotic lesions. Ann. N.Y. Acad. Sci. **748**, 501–507
7 Davenport, A. P., Kuc, R. E. and Mockridge, J. W. (1998) Endothelin-converting enzyme in the human vasculature: evidence for differential conversion of big endothelin-3 by endothelial and smooth-muscle cells. J. Cardiovasc. Pharm. **31**, S1–S3
8 Wang, H. and Keiser, J. A. (1998) Expression of membrane-type matrix metalloproteinase in rabbit neointimal tissue and its correlation with matrix-metalloproteinase-2 activation. J. Vasc. Res. **35**, 45–54
9 Lee, E., Grodzinsky, A. J., Libby, P., Clinton, S. K., Lark, M. W. and Lee, R. T. (1995) Human vascular smooth muscle cell-monocyte interactions and metalloproteinase secretion in culture. Arterioscl. Throm. Vas. Biol. **15**, 2284–2289
10 Wilhelm, S. M., Collier, I. E., Marmer, B. L., Eisen, A. Z., Grant, G. A. and Goldberg, G. I. (1989) SV40-transformed human lung fibroblasts secrete a 92-kDa type IV collagenase which is identical to that secreted by normal human macrophages. J. Biol. Chem. **264**, 17213–17221
11 Janusz, M. J., Hare, M., Durham, S. L., Potempa, J., McGraw, W., Pike, R., Travis, J. and Shapiro, S. D. (1999) Cartilage proteoglycan degradation by a mouse transformed macrophage cell line is mediated by macrophage metalloelastase. Inflamm. Res. **48**, 280–288
12 Vaalamo, M., Kariniemi, A. L., Shapiro, S. D. and Saarialho-Kere, U. (1999) Enhanced expression of human metalloelastase (MMP-12) in cutaneous granulomas and macrophage migration. J. Invest. Dermatol. **112**, 499–505
13 Xie, B., Dong, Z. and Fidler, I. J. (1994) Regulatory mechanisms for the expression of type IV collagenases/gelatinases in murine macrophages. J. Immunol. **152**, 3637–3644
14 Lindstedt, L., Saarinen, J., Kalkkinen, N., Welgus, H. and Kovanen, P. T. (1999) Matrix metalloproteinases-3, -7, and -12, but not -9, reduce high density lipoprotein-induced cholesterol efflux from human macrophage foam cells by truncation of the carboxyl terminus of apolipoprotein A-I. Parallel losses of pre-beta particles and the high affinity component of efflux. J. Biol. Chem. **274**, 22627–22634
15 Schumaker, V. N. and Puppione, D. L. (1986) Sequential flotation centrifugation. Methods Enzymol. **128**, 155–170
16 Skinner, E. R. (1992) The separation and analysis of high-density lipoprotein (HDL) and low-density lipoprotein (LDL) subfractions. In Lipoprotein Analysis: a Practical Approach (Converse, C. A. and Skinner, E. R., eds.), pp. 85–118, IRL Press, Oxford
17 Gianazza, E., Giacon, P., Sahlin, B. and Righetti, P. G. (1985) Non-linear pH courses with immobilized pH gradients. Electrophoresis **6**, 53–56
18 Schägger, H. and von Jagow, G. (1987) Tricine-sodium dodecyl sulfate-polyacrylamide gel electrophoresis for the separation of proteins in the range from 1 to 100 kDa. Anal. Biochem. **166**, 368–379
19 Link, A. J. (1998) 2-D Proteome Analysis Protocols, Humana Press, Totowa

20 Heukeshoven, J. and Dernick, R. (1986) Neue ergebnisse zum mechanismus der silberfärbung. In Elektrophorese Forum '86 (Radola, B. J., ed.), pp. 22–27, Technische Universitaet, Munich
21 Jeno, P., Mini, T., Moes, S., Hintermann, E. and Horst, M. (1995) Internal sequences from proteins digested in polyacrylamide gels. Anal. Biochem. **224**, 75–82
22 Wilm, M., Shevchenko, A., Houthaeve, T., Breit, S., Schweigerer, L., Fotsis, T. and Mann, M. (1996) Femtomole sequencing of proteins from polyacrylamide gels by nano-electrospray mass spectrometry. Nature (London) **379**, 466–469
23 Shevchenko, A., Wilm, M., Vorm, O. and Mann, M. (1996) Mass spectrometric sequencing of proteins from silver-stained polyacrylamide gels. Anal. Chem. **68**, 850–858
24 Vorm, O. and Mann, M. (1994) Improved mass accuracy in matrix-assisted laser desorption/ionization time-of flight mass spectrometry of peptides. J. Am. Soc. Mass Spectrom. **5**, 955–958
25 Takayama, M., Itoh, S., Nagasaki, T. and Tanimizu, I. (1977) A new enzymatic method for determination of serum cholin-containing phospholipids. Clin. Chim. Acta **79**, 93–96
26 Goetze, S., Xi, X. P., Kavano, Y., Kavano, H., Fleck, E., Hsueh, W. A. and Low, R. E. (1999) TNF-a-induced migration of vascular smooth muscle cells is MAPK dependent. Hypertension **33**, 183–189
27 Ghiselli, G., Rohde, M. F., Tanenbaum, S., Krishnan, S. and Gotto, A. M. (1985) Origin of apolipoprotein A-I polymorphism in plasma. J. Biol. Chem. **260**, 15662–15668
28 Lins, L., Piron, S., Conrath, K., Vanloo, B., Brasseur, R., Rosseneu, M., Baert, J. and Rusysschaert, J.-M. (1993) Enzymatic hydrolysis of reconstituted dimyristoylphosphatidylcholine-apo A-I complexes. Biochim. Biophys. Acta **1151**, 137–142
29 Roberts, L. M., Ray, M. J., Shih, T.-W., Hayden, E., Reader, M. M. and Brouillette, C. G. (1997) Structural analysis of apolipoprotein A-I: limited proteolysis of methionine-reduced and -oxidized lipid-free and lipid-bound human apo A-I. Biochemistry **36**, 7615–7624
30 Kunitake, S. T., Chen, G. C., Kung, S. F., Schilling, J. W., Hardman, D. A. and Kane, J. P. (1990) Pre-b high density lipoprotein: unique disposition of apolipoprotein A-I increases susceptibility to proteolysis. Arteriosclerosis **10**, 25–30
31 Dalton, M. B. and Swaney, J. B. (1993) Structural and functional domains of apolipoprotein A-I within high density lipoproteins. J. Biol. Chem. **268**, 19274–19283
32 Calabresi, L., Tedeschi, G., Treu, C., Ronchi, S., Galbiati, D., Airoldi, S., Sirtori, C. R., Marcel, Y. and Franceschini, G. (2001) Limited proteolysis of a disulfide-linked apoA-I dimer in reconstituted HDL. J. Lipid Res. **42**, 935–942
33 Ji, Y. and Jonas, A. (1995) Properties of an N-terminal proteolytic fragment of apolipoprotein A-I in solution and in reconstituted high density lipoproteins. J. Biol. Chem. **270**, 11290–11297
34 Murphy, G. (1990) Purification of connective tissue metalloproteinases. In Protein Purification Applications: a Practical Approach (Harris, E. L. V. and Angal, S., eds.), pp. 142–146, IRL Press, Oxford
35 Ross, R. (1993) The pathogenesis of atherosclerosis: a perspective for the 1990s. Nature (London) **362**, 801–809
36 Castro, G. R. and Fielding, C. J. (1988) Early incorporation of cell-derived cholesterol into pre-b-migrating high-density lipoprotein. Biochemistry **27**, 25–29
37 Yancey, P. G., Bielicki, J. K., Johnson, W. J., Lund-Katz, S., Palgunachari, M. N., Anantharamaiah, G. M., Segrest, J. P., Phillips, M. C. and Rothblat, G. H. (1995) Efflux of cellular cholesterol and phospholipid to lipid-free apolipoproteins and class A amphipatic peptides. Biochemistry **34**, 7955–7965
38 Sviridov, D., Pyle, L. E. and Fidge, N. (1996) Efflux of cellular cholesterol and phospholipid to apolipoprotein A-I mutants. J. Biol. Chem. **271**, 33277–33283
39 Phillips, J. C., Wriggers, W., Li, Z., Jonas, A. and Schulten, K. (1997) Predicting the structure of apolipoprotein A-I in reconstituted high-density lipoprotein disks. Biophys. J. **73**, 2337–2346
40 Segrest, J. P., Jones, M. K., Klon, A. E., Sheldahl, C. J., Hellinger, M., De Loof, H. and Harvey, S. C. (1999) A detailed molecular belt model for apolipoprotein A-I in discoidal high density lipoprotein. J. Biol. Chem. **274**, 31755–31758
41 Tricerri, M. A., Behling Agree, A. K., Sanchez, S. A., Bronski, J. and Jonas, A. (2001) Arrangement of apolipoprotein A-I in reconstituted high-density lipoprotein disks: an alternative model based on fluorescence resonance energy transfer experiments. Biochemistry **40**, 5065–5074
42 Wang, G., Sparrow, J. T. and Cushley, R. J. (1997) The helix-hinge motif in human apolipoprotein A-I determined by NMR spectroscopy. Biochemistry **36**, 13657–13666
43 Borhani, D. W., Rogers, D., Engler, J. A. and Brouillette, C. G. (1997) Crystal structure of truncated apolipoprotein A-I suggests a lipid-bound conformation. Proc. Natl. Acad. Sci. U.S.A. **94**, 12291–12296
44 Borhani, D. W., Engler, J. A. and Brouillette, C. G. (1999) Crystallization of truncated human apolipoprotein A-I in a novel conformation. Acta Crystallogr. D. Biol. Crystallogr. **55**, 1578–1583
45 Brouillette, C. G., Anantharamaiah, G. M., Engler, J. A. and Borhani, D. W. (2001) Structural models of human apoliporotein A-I: a critical analysis and review. Biochim. Biophys. Acta **1531**, 4–46
46 Okon, M., Frank, P. G., Marcel, Y. L. and Cushley, R. J. (2001) Secondary structure of human apolipoprotein A-I(1–186) in lipid-mimetic solution. FEBS Lett. **487**, 390–396
47 Segrest, J. P., Jackson, R. L., Morrisett, J. D. and Gotto, A. M. J. (1974) A molecular theory of lipid-protein interactions in the plasma lipoproteins. FEBS Lett. **38**, 247–258
48 Laccotripe, M., Makrides, S. C., Jonas, A. and Zannis, V. I. (1997) The carboxyl terminal hydrophobic residues of apolipoprotein A-I affect its rate of phospholipid binding and its association with high density lipoprotein. J. Biol. Chem. **272**, 17511–17522

Received 16 October 2001/10 December 2001; accepted 7 January 2002